Electronic Supplementary Material (ESI) for ChemComm.

SUPPORTING INFORMATION

Use of Redox Probe for Electrochemical RNA-ligand Binding Assay in Microliter Droplets

Hélène Guyon,[a,b] François Mavré,[b] Marjorie Catala,[c] Serge Turcaud,[a] Franck Brachet,[c] Benoît Limoges,[b*] Carine Tisné,[c*] and Laurent Micouin[a*]

[a] *Laboratoire de Chimie et Biochimie pharmacologiques et toxicologiques, UMR 8601 CNRS, Université Paris Descartes, Sorbonne Paris Cité, UFR Biomédicale, 45 rue des Saints Pères, 75006 Paris, France.*

[b] *Laboratoire d'Electrochimie Moléculaire, UMR 7591 CNRS, Université Paris Diderot, Sorbonne Paris Cité, 15 rue Jean-Antoine de Baïf, 75205 Paris, France.*

[c] *Laboratoire de Cristallographie et RMN biologiques, UMR 8015, CNRS, Université Paris Descartes, Sorbonne Paris Cité, Faculté de Pharmacie, 4 av. de l'Observatoire, 75006 Paris, France.*

CHEMISTRY

Synthesis of ferrocene-paromomycin (FcPRM)

All reagents and solvents were purchased from chemical suppliers and used without further purification. Analytical thin layer chromatography (TLC) was performed on commercially available silica gel plates $60F_{254}$ and revealed by phosphomolybdic acid or ninhydrin stains. Flash column chromatography was performed on silica gel 60 (40-63 µM). NMR spectra were recorded on a 500 MHz Bruker Avance spectrometer. Chemical shifts (δ) are reported in ppm relative to the residual solvent peak for ^{1}H NMR: D_2O (δ 4.79). Coupling constants (*J*) are reported in Hertz unit (Hz). Multiplicities are described with the following abbreviations: s = singlet, br = broad, d = doublet, t = triplet, q = quadruplet, m = multiplet. Low resolution mass spectra (LRMS) were recorded with an ion trap mass analyzer under electrospray ionization (ESI) in positive mode detection.

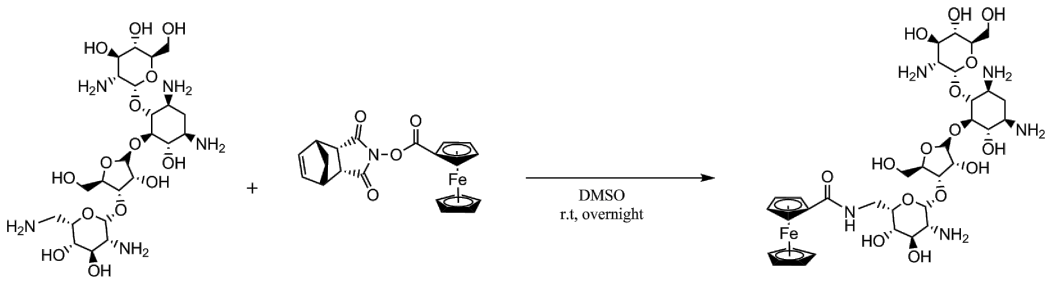

Scheme 1.

Paromomycin free base (940 mg, 1.5 mmol, 1 equiv.) was first dissolved in DMSO (15 mL). In parallel, Fc-NBD (475 mg, 1.2 mmol, 0.8 equiv.) was dissolved in DMSO (15 mL). The two solutions were then combined and the resulting orange mixture was stirred at room temperature overnight. Conversion was followed by TLC (2:2:1 volumetric ratio for $CHCl_3$/MeOH/NH_4OH). The reaction mixture was evaporated under reduced pressure, yielding a brown oil. Water (100 mL) was added to the resulting residue and freeze-dried to give rise to an orange crude. The crude was purified by flash column chromatography using $CHCl_3$/MeOH/NH_4OH as eluent (2:2:1). The corresponding fractions were combined, evaporated and finally lyophilized to remove any trace of water and gave rise to an orange solid (317 mg, 0.38 mmol, yield = 32 %).

TLC Rf: 0.35
^{1}H NMR (D_2O, 500 MHz, 313 K): δ 5.73 (s, H1'), δ 5.35 (s, H1"), δ 5.25 (s, H1'''), δ 4.86 (s, H3'''', H1''''), δ 4.61 (s, H2'''', H4''''), δ 4.43 (t, *J* = 5.2 Hz, H3"), δ 4.35 (s, H2"), δ 4.34 (s, 5H*'''''), δ 4.30 (t, *J* = 5.4 Hz, H3'''), δ 4.24 (m, H4''), δ 4.22 (s, H5'''), δ 3.97 (dd, *J* = 10.5 Hz and 4.6 Hz, H6'b), δ 3.96 (s, H3'), δ 3.89 (m, H5, H6), δ 3.88 (s, H5''b), δ 3.81 (m,

H4’’’, H5’), δ 3.80 (s, H6’a), δ 3.69 (m, H6’’’b, H5’’a), δ 3.61 (s, H2’’’), δ 3.60 (s, H6’’’a), δ 3.55 (t, *J* = 9.5 Hz, H4), δ 3.51 (t, *J* = 9.3 Hz, H4’), δ 3.50 (s, H1), δ 3.40 (dd, *J* = 10.8 Hz, and 3.7 Hz, H2’), δ 3.34 (m, H3), δ 2.49 (d, *J* = 13.0 Hz, H2b), δ 1.80 (q, *J* = 12.5 Hz, H2a).

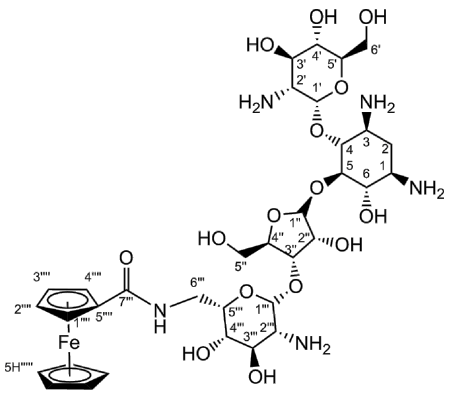

FcPRM

^{13}C NMR (D_2O, 125 MHz, 313 K): δ 177.60 (C7’’’), δ 99.0 (C1’), δ 98.80 (C1’’’), δ 98.60 (C1’’), δ 87.70 (C5), δ 84.80 (C4’’), δ 80.70 (C6), δ 78.80 (C3’’), δ 76.90 (C5’, C5’’’’), δ 76.60 (C2’’), δ 76.20 (C5’’’), δ 75.60 (C4), δ 74.85 (C2’’’’, C4’’’’), δ 73.30 (5C*’’’’’), δ 72.50 (C4’), δ 72.00 (C3’), δ 71.80 (C3’’’’), δ 71.30 (C1’’’’), δ 70.80 (C3’’’), δ 69.80 (C4’’’), δ 63.82 (C5’’), δ 63.62 (C6’), δ 57.03 (C2’), δ 54.32 (C2’’’), δ 53.00 (C3), δ 52.00 (C1), δ 43.10 (C6’’’), δ 31.68 (C2).

ESI MS: [MH^+] 828.5

BIOLOGICALS

Samples preparation

Chemically synthesized and deprotected 16S23 RNA representing the 16S bacterial A site (Figure S1) was purchased from GE Healthcare Life Sciences. 16S23 RNA was diluted to 1 mM concentration in 10 mM MES pH 5.5, 150 mM NaCl and 0.1 mM EDTA (buffer 1), heated at 95°C for 1 min and then cooled on ice for 5 min. Correct folding was checked by SDS-PAGE gel (18 %). For ITC and electrochemical experiments, RNA samples were dialyzed against buffer 1.

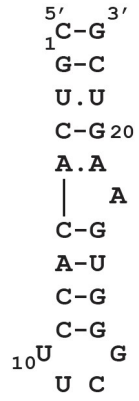

16S23 RNA

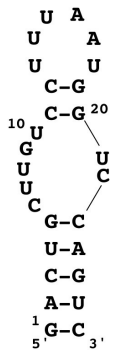

Neomycin riboswitch

Figure S1. Sequences of 16S23 RNA mimicking the 16S bacterial A site and of the neomycin riboswitch used in this study.

Determination of the dissociation constant between FcPRM and 16S23 RNA

The dissociation constant between the ferrocenyl-labeled paromomycin and 16S23 RNA was determined both by cyclic voltammetry and isothermal titration microcalorimetry (ITC).

K_D determination by cyclic voltammetry

Cyclic voltammetric measurements were performed with a CHI 900 potentiostat and the data were acquired using a CHI 900 software. All electrochemical experiments were performed with disposable arrays of ten miniaturized electrochemical cells made of three electrodes (a carbon-based working electrode of 0.0177 cm^2, a carbon-based counter electrode, and an Ag/AgCl-based reference electrode) screen-printed on a planar polyethylene terephthalate film. A DEK-model 65 semiautomatic screen-printer (Presco, USA) was used to deposit the successive thick film layers. The working and counter carbon-based electrodes were printed from the commercial carbon-based ink Electrodag PF-470 (Acheson Colloid Co.), while the silver-based pseudo-reference electrode from the silver-based ink Electrodag 418SS (Acheson Colloid Co.). A last layer of curable dielectric thick film (Vinilfast 36, Kiian, Italy) was screen-printed over the electrodes in such a way to generate circular three-electrode electrochemical microcells (circular wells of 5-mm diameter) and to insulate a part of the conductive paths of the electrodes. On account of the hydrophobic nature of the circular insulating layer, it enables to maintain in place a hemispherical droplet solution of less than 50 µL. Electrochemical experiments were all performed in buffer 1 and at room temperature (~20°C).

Before each experiment, screen-printed carbon electrodes were carefully washed in absolute ethanol for 15 min, then rinsed with ultrapure water and next coated with a layer of bovine serum albumin (BSA) by spreading a 50-µL droplet of 0.1 % wt BSA in water over each individual electrochemical cell for 15 min. The BSA coating was shown to reduce the nonspecific adsorption on the electrode surface, leading thus to more reproducible results. After BSA-coating and before their use in RNA binding assays, the electrodes were thoroughly washed twice with ultrapure water and then controlled by CV in buffer 1 (i.e., by doing a CV scan from 0.1 V to 0.7 V *vs.* Ag/AgCl at a scan rate v = 0.1 V/s).

Titrations of FcPRM by 16S23 RNA in buffer 1 were performed as follow. To a 38.5 µL-droplet solution containing a starting concentration of FcPRM in buffer 1, small aliquots of 16S23 RNA (*i.e.*, 0.2 to 0.8 µL of different stock solutions of RNA) were incrementally injected and mixed into the droplet in such a way to rise the RNA concentration from 0.07 to

8.3 equivalents. After each injection, a series of CVs were performed until complete stabilization of the voltammetric response was observed. The anodic peak current (I) of the last recorded CV was used as the analytical response. After correction from dilutions and normalization to the starting peak current value (I_{free}), it was then plotted as a function of the RNA concentration. Dissociation constant values (K_D) were recovered from non-linear least square fitting of eq S1 to the normalized data of the titration plots:

$$\frac{I}{I_{free}} = \sqrt{\left(1-\frac{K_D+[\mathrm{FcPRM}]+[\mathrm{RNA}]-\sqrt{(K_D+[\mathrm{FcPRM}]+[\mathrm{RNA}])^2-4[\mathrm{FcPRM}][\mathrm{RNA}]}}{2[\mathrm{FcPRM}]}\right)\left(1-\left(\frac{I_{bound}}{I_{free}}\right)^2\right)+\left(\frac{I_{bound}}{I_{free}}\right)^2} \quad \text{(S1)}$$

where I is the magnitude of the peak current of FcPRM at a given concentration of RNA, I_{bound} the peak current intensity at an extrapolated infinite concentration of RNA, [FcPRM] and [RNA] the total concentrations of FcPRM and RNA, respectively, in the droplet. This equation is valid for a 1:1 binding stoichiometry between FcPRM and 16S23 RNA, and under the assumption of a dynamic equilibrium between the free and bound reduced form of FcPRM, but also its oxidized form, on the time scale of the CV experiments (*i.e.* chemical reactions are considered as fast and always at equilibrium when compared to the electron transfer kinetics. See A. De Rache *et al.*, *J. Electroanal. Chem.* **2015**, *745*, 44-45). In order to verify this assumption, we attempted to determine the second order association rate constant between FcPRM and 16S23 RNA using our previously kinetic rotating droplet electrochemical method (L. Challier *et al.*, *J. Am. Chem. Soc.* **2013**, *135*, 14215-14228). Even though we were unable to accurately determine its absolute value because of its too fast rate compared to the time resolution of our method, we were nevertheless able to ascertain that it is superior to 10^5 $M^{-1}s^{-1}$. Such a value agree with a dynamic equilibrium on the time scale of the CV experiments and so validate the use of eq S1 for the determination of K_D. From the fit of eq S1 to the 3 independent titration curves shown in Figure S2, an average K_D value of (7.8 ± 1.4) μM was inferred.

A

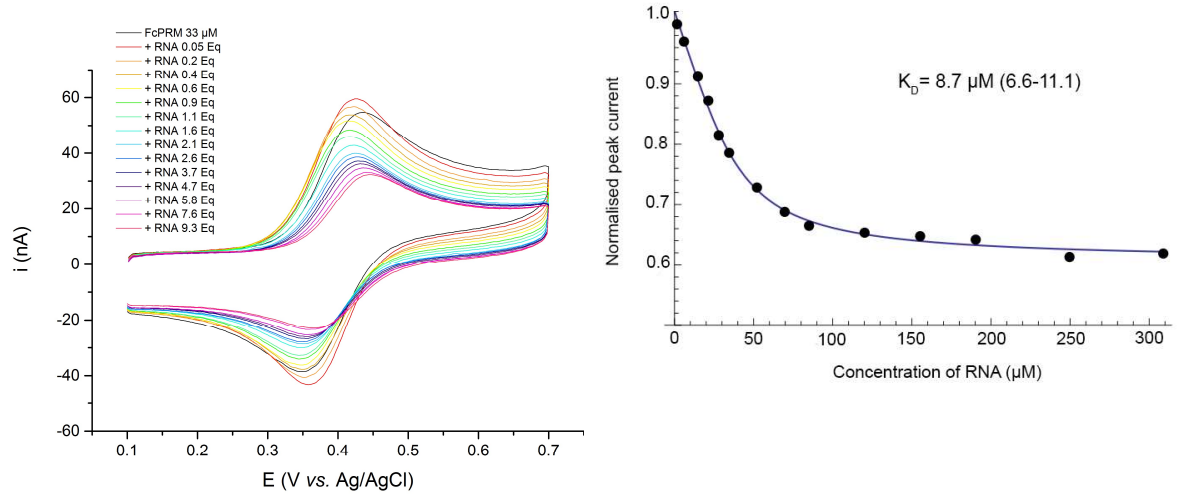

B

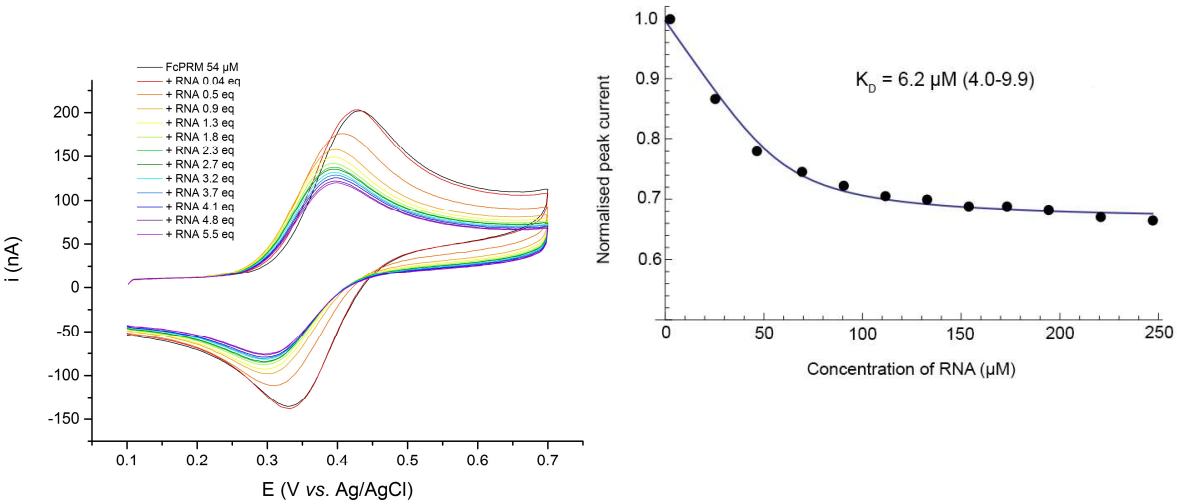

C

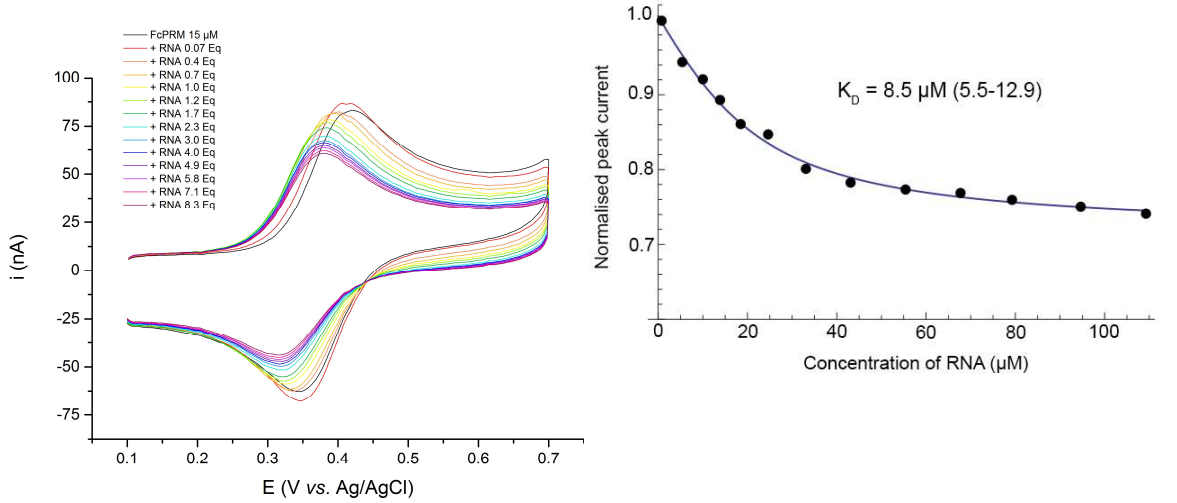

Figure S2. (Left) Experimental CVs and (right) corresponding titration curves of FcPRM by 16S23 RNA. The starting concentration of FcPRM for each titration was: (A) 33 µM, (B) 54 µM, and (C) 15 µM. The plain line corresponds to the non-linear least-square fit of eq S1 to the data. K_D value recovered from the fit is indicated on the graph with a 95% confidence interval in bracket.

K_D determination by Isothermal titration microcalorimetry

Titrations were conducted at 25°C with the 16S23 RNA in the cell of a MicroCal ITC200 (GE Healthcare Lifesciences) at a concentration of 100 µM and FcPRM at a concentration of 1.5 mM in the seringe. 25 injections of 1.54 µL of FcPRM were made at a stirring of 1000 rpm with 180 s between injections. Before the experiments, the RNA sample was extensively dialysed against buffer 1 and the dialysis buffer was used to dissolve FcPRM. ITC curves (Figure S3) were analysed using the software Origin 7.0 (OriginLab) using a model with two-sequential-binding sets of sites to take into account unspecific binding commonly occurring with aminoglycoside-type compounds.

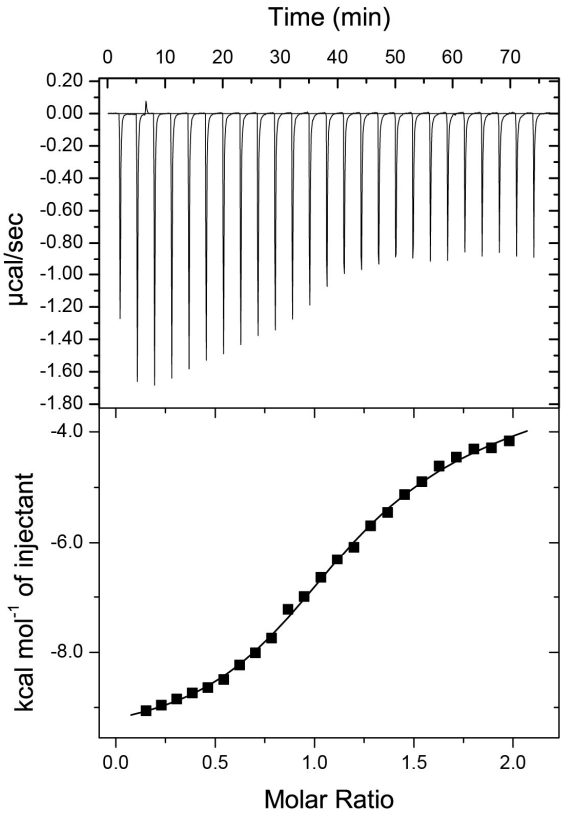

Figure S3. ITC experiment showing the binding of FcPRM to the 16S23 RNA. The binding parameters are reported in Table S1.The titration thermogram is represented as heat per unit of time released after each injection of the ligand into the protein (top graph). The area of each peak is then integrated and plotted versus the molar ratio of the ligand concentration and total RNA concentration. The resulting isotherm obtained was then fitted to a binding model with two-sequential binding sites to take into account the unspecific binding due to electrostatic interactions between RNA and aminoglycoside (bottom graph).

Table S1. Binding of FcPRM to the 16S23 RNA

	K_D (μM)	N	ΔH (kcal/mol)	-TΔS (kcal/mol)
16S23 RNA specific binding site	9.3	1.1	-9.6	2.7

The K_D value measured by ITC is found within the intervals of confidence of K_D determined by cyclic voltammetry.

NMR analysis of FcPRM binding to 16S23 RNA

The analysis of the FcPRM binding on 16S23 was monitored by NMR using two different experiments: (i) 1D NMR spectra recorded on an RNA sample in 95% ^1H_2O, 5% D_2O in order to observe imino protons (Figure S4 A) and (ii) TOSCY experiment with a mixing time of 45 ms recorded on an RNA sample in fully deuterated buffer in order to observe H5-H6 correlation peaks from C and U nucleotides (Figure S4 B). In both cases, the 16S23 RNA was prepared in the NMR buffer containing 10 mM KPO_4, pH 6.5 and 50 mM KCl. A reference spectrum was recorded with the 16S23 RNA alone in the NMR tube and then the same spectrum was recorded upon addition of FcPRM (Figure S4 A and B). The 16S RNA protons were previously assigned (T. Lombès et al, *Angew. Chem. Int. Ed.* **2012**, *51*, 9530-9534). The NMR chemical shift mapping shows that FcPRM has the same binding site than paromomycin on 16S23 RNA.

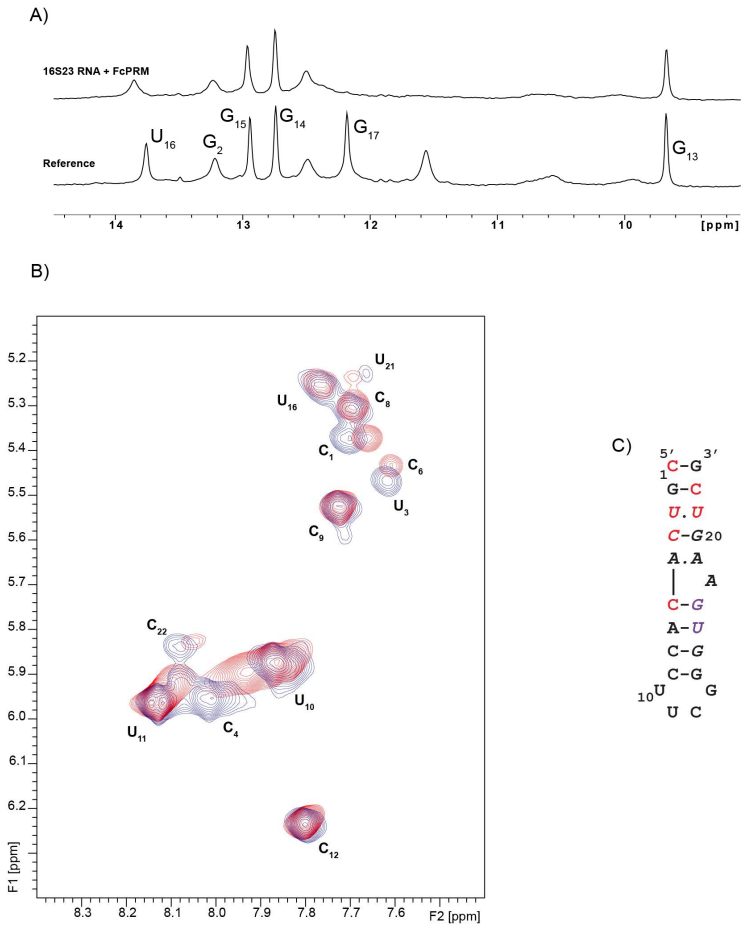

Figure S4. (A) ^{1}H spectrum of 16S23 RNA (0.38 mM) alone in KPO_4 buffer pH 6.5 containing 50 mM KCl, at 288 K with FcPRM probe (1 equivalent), (B) TOCSY experiments recorded in deuterated buffer showing the chemical shift variations in the region of H5-H6 protons of 16S23 RNA alone (in blue) and in the presence of FcPRM (in red, 2 equivalents) (C) Chemical shift mapping showing the binding site of FcPRM on 16S23 RNA, in red from results of B and in purple from A, nucleotides in italic are those involved in binding of 16S23 RNA by paromomycin (Fourmy et al. *J. Mol. Biol.* **1998**, *277*, 347-362).

Characterization of different aminoglycosides for their binding to 16S23 RNA through electrochemical competitive binding assay

The dissociation constants of three aminoglycosides, *i.e.* paromomycin, neomycin and neamine, to 16S23 RNA were determined by competitive electrochemical binding experiments.

To a 39.2 µL-droplet solution containing a pre-equilibrated mixture of FcPRM and 16S23 RNA (1:0.8 ratio) in buffer 1, increasing amounts of aminoglycoside (from 0.1 to 5.2 equivalents) were injected with a micropipette into the droplet (*i.e.*, 0.2 to 0.8 µL of different stock solutions of aminoglycoside) and mixed. After each injection, CVs were cycled until complete stabilization of the current response was observed. The anodic peak current of the last recorded CV was used as the analytical response (*I*) and, after correction from dilutions

and normalization to the starting peak current value (I_{free}), then plotted as a function of the RNA concentration.

Dissociation constants of the aminoglycoside competitors (K_D) were recovered from the non-linear least square fit of eq S2 to the electrochemical competitive binding curves using a K_D^{FcPRM} value of 7.8 μM.

$$\frac{I}{I_{free}} = \sqrt{1-\left(\frac{2\sqrt{a^2-3b}\cos(\theta/3)-a}{3K_D+2\sqrt{a^2-3b}\cos(\theta/3)-a}\right)\left(1-\left(\frac{I_{bound}}{I_{free}}\right)^2\right)} \qquad \text{(S2)}$$

where $\theta = arc\cos\left[\frac{-2a^2+9ab-27c}{2\sqrt{\left(a^2-3b\right)^3}}\right]$

$a = K_D^{FcPRM} + K_D + [FcPRM] + [C] - [RNA]$

$b = \{[C]-[RNA]\}K_D^{FcPRM} + \{[FcPRM]-[RNA]\}K_D + K_D^{FcPRM}K_D$

$c = -K_D^{FcPRM}K_D[RNA]$

where K_D^{FcPRM} and K_D are the dissociation constants of the FcPRM probe and the aminoglycoside competitor, respectively, [FcPRM] and [C] are the total concentrations of FcPRM and competitor, respectively, and [RNA] is the total concentration of 16S23 RNA initially added to the droplet solution. I_{free} is the initial peak current recorded when there is neither RNA nor competitor added to the droplet solution, whereas I_{bound} is the peak current at an extrapolated infinite concentration of RNA in the absence of competitor. K_D^{FcPRM}, [FcPRM] and [RNA] were given as known data in eq S2.

Neomycin

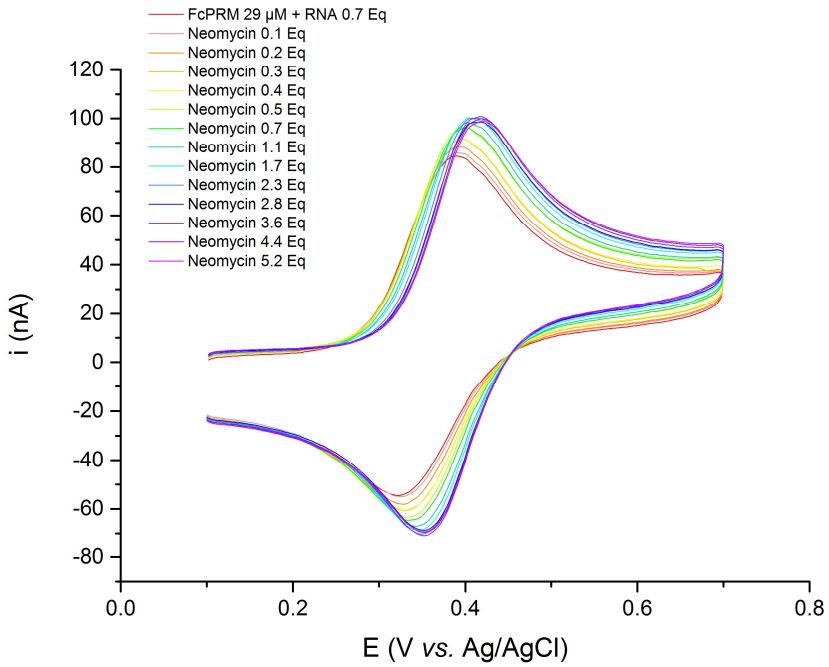

Figure S5. CVs of the competitive binding assay with neomycin. The starting concentrations were: [FcPRM] = 29 µM and [16S23 RNA] = 20 µM.

Paromomycin

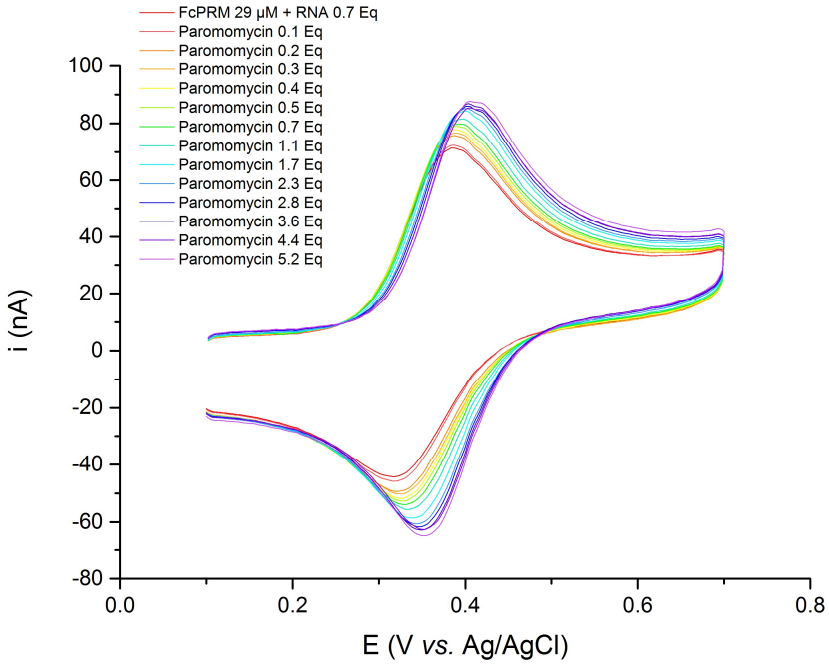

Figure S6. CVs of the competitive binding assay with paromomycin. The starting concentrations were: [FcPRM] = 29 µM and [16S23 RNA] = 20 µM.

Neamine

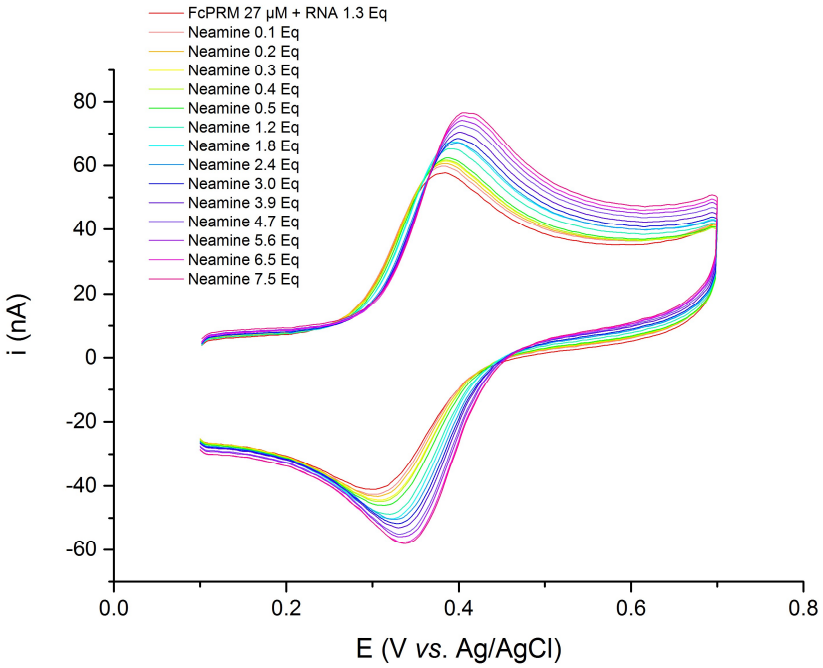

Figure S7. CVs of the competitive binding assay with neamine. The starting concentrations were: [FcPRM] = 27 µM and [16S23 RNA] = 35 µM.

NMR analysis of FcPRM binding to neomycin riboswitch

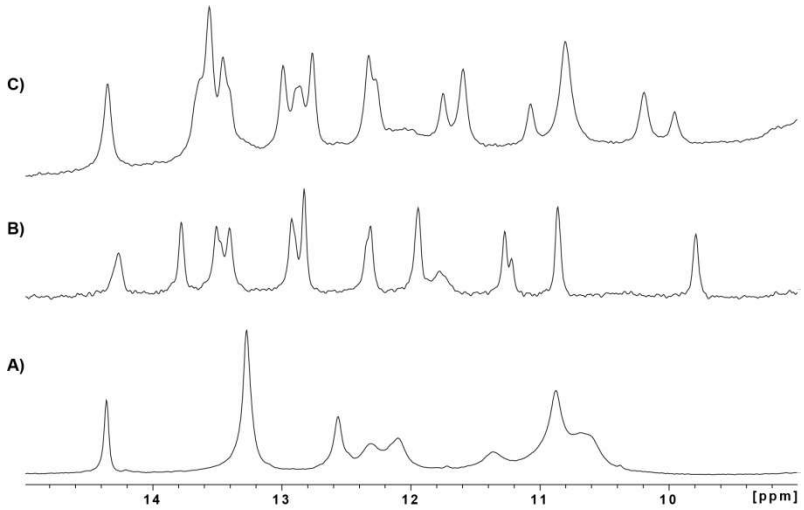

Figure S8. ^{1}H NMR spectra of neomycin riboswitch (Neo-switch, 0.4 mM). (A) alone, (B) with one equivalent of neomycin, and (C) with one equivalent of FcPRM probe **4**. The spectra were recorded in KPO_4 buffer pH 6.5 containing 50 mM KCl and at 288 K.

Figure S8 C shows the 1D NMR spectrum of the imino protons of Neo-switch upon addition of FcPRM. Its comparison to the spectra of the free riboswitch (Figure S8 A) together with that upon binding of neomycin (Figure S8 B) shows that FcPRM binds to Neo-switch and

does not prevent its folding. Indeed, the addition of FcPRM in the Neo-switch sample provokes the apparition of new and sharp NMR signals of imino protons that corresponds to the folding of the riboswitch upon binding. The spectrum is different from that of Neo-switch with neomycin due to chemical differences of FcPRM compared to neomycin that change the chemical shifts of the Neo-switch imino protons in the bound form.

Determination of K_D between FcPRM and neomycin riboswitch

The titration procedure was similar than for FcPRM with 16S23 RNA.

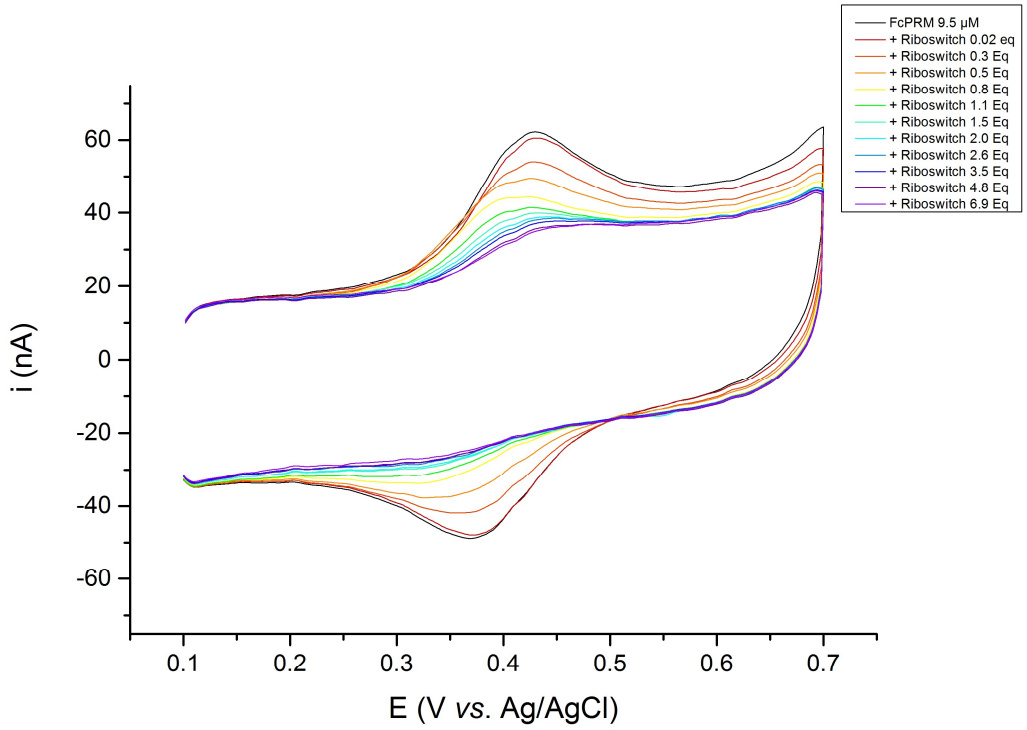

Figure S9. (A) Experimental CVs and (B) corresponding titration curves of FcPRM by neomycin riboswitch. The starting concentration of FcPRM was 9.5 µM.

Competitive assay between FcPRM and neomycin with neomycin riboswitch.

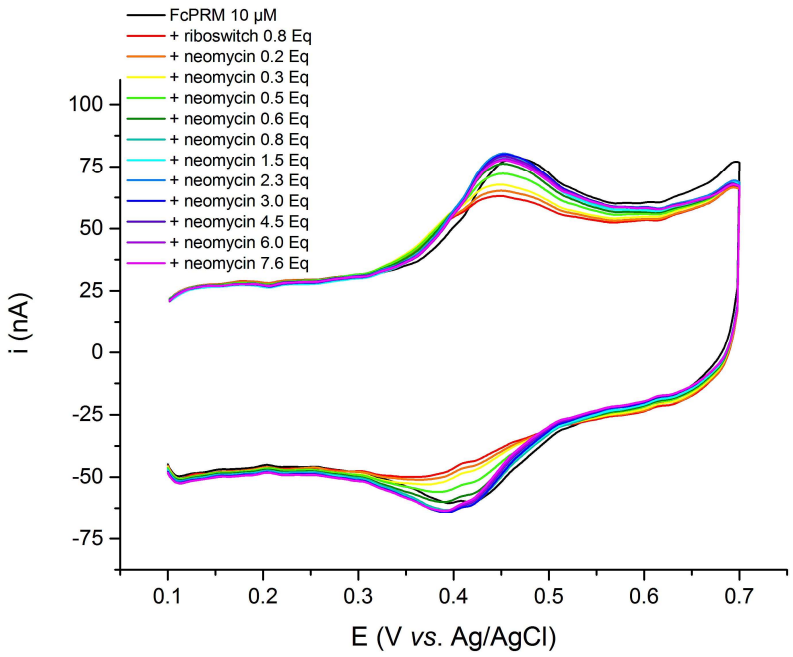

Figure S10. Electrochemical competitive binding assay of neomycin. Cyclic voltammograms (v = 0.1 $V.s^{-1}$) recorded for increasing concentrations of neomycin to a solution of FcPRM/Neo-switch complex. The concentrations of FcPRM and Neo-switch were 10 µM and 8 µM, respectively.